Natural Product Reports

ROYAL SOCIETY OF CHEMISTRY

REVIEW

View Article Online
View Journal

Cite this: DOI: 10.1039/d6np00014b

Inverse stable isotopic labeling for natural product characterization and discovery

Jose Miguel D. Robes and Aaron W. Puri *

Covering: 2005 to 2026

Stable isotopic labeling is a powerful tool in natural products research; however, the isotopically substituted precursors required for conventional labeling approaches are not always available. In such cases, inverse stable isotopic labeling (InverSIL) offers an effective alternative. In this approach, natural product producing organisms are grown on isotopically substituted media, which is then supplemented with precursors at their natural isotopic abundance. Incorporation of these unlabeled precursors can be readily detected due to their isotopic contrast, circumventing limitations associated with precursor availability. Here, we review applications of InverSIL in the characterization of natural product biosynthetic pathways and structures, as well as its use in genome mining to link biosynthetic genes to the natural products they produce. We also discuss contexts in which the InverSIL approach is particularly advantageous, as well as situations where its utility may be limited. Through this review, we aim to encourage broader adoption of InverSIL as a versatile strategy for advancing natural products research.

Received 3rd February 2026

DOI: 10.1039/d6np00014b

rsc.li/npr

Department of Chemistry and the Henry Eyring Center for Cell and Genome Science, University of Utah, Salt Lake City, UT 84112, Utah, USA. E-mail: a.puri@utah.edu; Tel: (801) 213-1408

1. Introduction

The assembly of natural products, also known as secondary or specialized metabolites, is genetically encoded. Consequently, many natural products have potent biological activities because their structures have been under selection for millennia. For this reason, natural products have been the basis for most small molecule therapeutics,[1] and there is a constant demand for the discovery of new natural products. Understanding the biosynthesis of these molecules can also unveil new biochemical transformations that may be useful for future medicinal chemistry efforts.[2,3]

Stable isotopes, which are non-radioactive forms of elements that differ in their number of neutrons, have been a key part of understanding the enzymatic transformations involved in natural product biosynthesis.[4,5] Modern advances in analytical methods, including mass spectrometry and nuclear magnetic resonance (NMR) spectroscopy, have enabled natural products containing naturally less abundant stable isotopes to be detected with ease, even though the structures of these variants are the same. This makes stable isotopes the "ultimate labels" for tracking the fate of molecules, although non-trivial changes in chemical properties (*e.g.* kinetic isotope effects) should not be ignored.

An isotopically substituted compound is defined as one in which virtually all of one element in the compound is a single isotope.[6] This is indicated with parentheses; for example, (1-^{13}C) glucose contains virtually only ^{13}C at the C1 position, while ($^{13}C_6$)glucose contains virtually only ^{13}C at all six carbon positions. In contrast, an isotopically labeled compound contains a mixture of isotopes for a given element but is specifically enriched for a certain isotope. This is indicated with square brackets. Here, we refer to a culture or organism that has been grown on an isotopically substituted element as "isotopically labeled" because it is not known whether every metabolite in the culture has been completely substituted. When strictly following the nomenclature of the International Union of Pure and Applied Chemistry (IUPAC),[6] an unlabeled compound (one at its natural isotopic abundance) should not have a prefix. For example, unlabeled glucose is different from ($^{12}C_6$)glucose, where the former contains approximately 98% ^{12}C, while the latter contains virtually only ^{12}C at each position. For simplicity, the figures in this review depict unlabeled compounds as only containing the most naturally abundant isotope (*e.g.* ^{12}C).

Natural products can be divided into various compound classes. Most of the examples discussed in this review belong to two major classes of natural products: polyketides and peptide-derived natural products. Polyketides are made by multidomain enzymes called polyketide synthases (PKSs), and their biosynthesis is mechanistically similar to fatty acid synthesis.[7] Polyketide biosynthesis begins with an activated starter unit (often acetyl-CoA or propionyl-CoA), which is then built upon in an assembly line fashion. The acyltransferase (AT) domain transfers the starter unit to the phosphopantetheine group of the acyl carrier protein (ACP). This is then transferred to the ketosynthase (KS) domain followed by the stepwise addition of extender units *via* a decarboxylative Claisen-like condensation between the starter unit and the next ACP-tethered extender unit in an iterative or modular manner (Fig. 1A). Structural complexity in these natural products comes from building block variation and backbone modification by additional PKS domains during chain elongation.[4]

There are two main classes of peptide-derived natural products: non-ribosomal peptides and ribosomally synthesized and post-translationally modified peptides (RiPPs). Similar to PKSs, non-ribosomal peptide synthetases (NRPSs) are organized into modules containing essential domains that catalyze peptide biosynthesis in an assembly line fashion. The adenylation (A) domain selects and activates the α-carboxyl group of a specific proteinogenic or non-proteinogenic amino acid. The activated amino acid is then transferred to the phosphopantetheine group of the peptidyl carrier protein (PCP), and the condensation (C) domain subsequently catalyzes peptide bond formation between amino acids in adjacent modules (Fig. 1B). This process can also include modification modules, such as epimerization domains, resulting in increased structural diversity.[8]

In contrast, RiPPs are genetically encoded peptides, and their biosynthesis is limited to the 20 proteinogenic amino acids. RiPP structural diversity is generated by the variety of post-translational modifications by RiPP maturases.[9] Briefly, a precursor peptide containing a leader sequence for enzyme recognition and a core peptide is translated and post-translationally modified by one or more RiPP maturases, and the leader sequence is subsequently cleaved by a protease, yielding the modified core peptide as the final product (Fig. 1C).

One of the largest drawbacks of isotopic labeling experiments is that access to isotopically labeled precursors is often limited. However, the ability to uniformly label microorganisms with stable isotopes (most commonly ^{13}C or ^{15}N) has enabled inverse stable isotopic labeling (InverSIL) as an alternative approach. In this technique, an organism is fully labeled by culturing it in media where one element is only available in an isotopically substituted form (*e.g.* ^{13}C or ^{15}N). Subsequently,

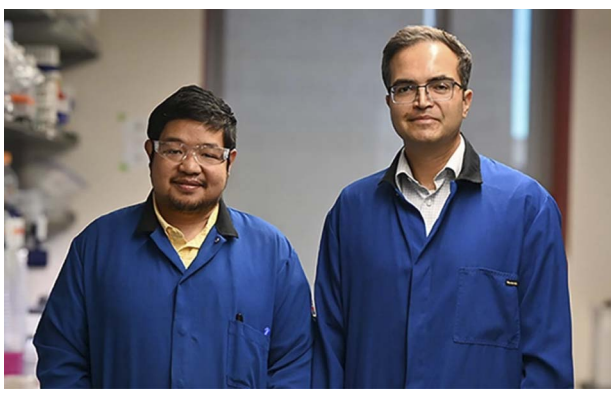

Jose Miguel D. Robes (left) Aaron W. Puri (right)

Jose Miguel D. Robes (left) obtained his B.S. in Biology from the University of the Philippines Baguio. He then worked as a research associate in the laboratory of Professor Gisela Concepcion at the Marine Science Institute, University of the Philippines Diliman, where he studied natural products from mollusk-associated bacteria. He subsequently joined the laboratory of Professor Aaron Puri at the University of Utah, where he received his PhD in Chemistry in 2025. He is currently undertaking postdoctoral training in the same lab on peptide natural products from methane-oxidizing bacteria. Aaron W. Puri (right) obtained his PhD in Chemical & Systems Biology from Stanford University working in Matt Bogyo's lab, where he developed and applied chemical tools to dissect host–pathogen interactions involving enteric bacteria. He then did his postdoctoral research at the University of Washington, where he was co-mentored by Mary Lidstrom and Pete Greenberg and worked on genetic tools and chemical signaling in methane-oxidizing bacteria. He has been an assistant professor at the University of Utah in the Department of Chemistry and the Henry Eyring Center for Cell and Genome Science since 2019. The Puri Lab focuses on understanding how underexplored bacteria use natural products to interact with each other and their environment.

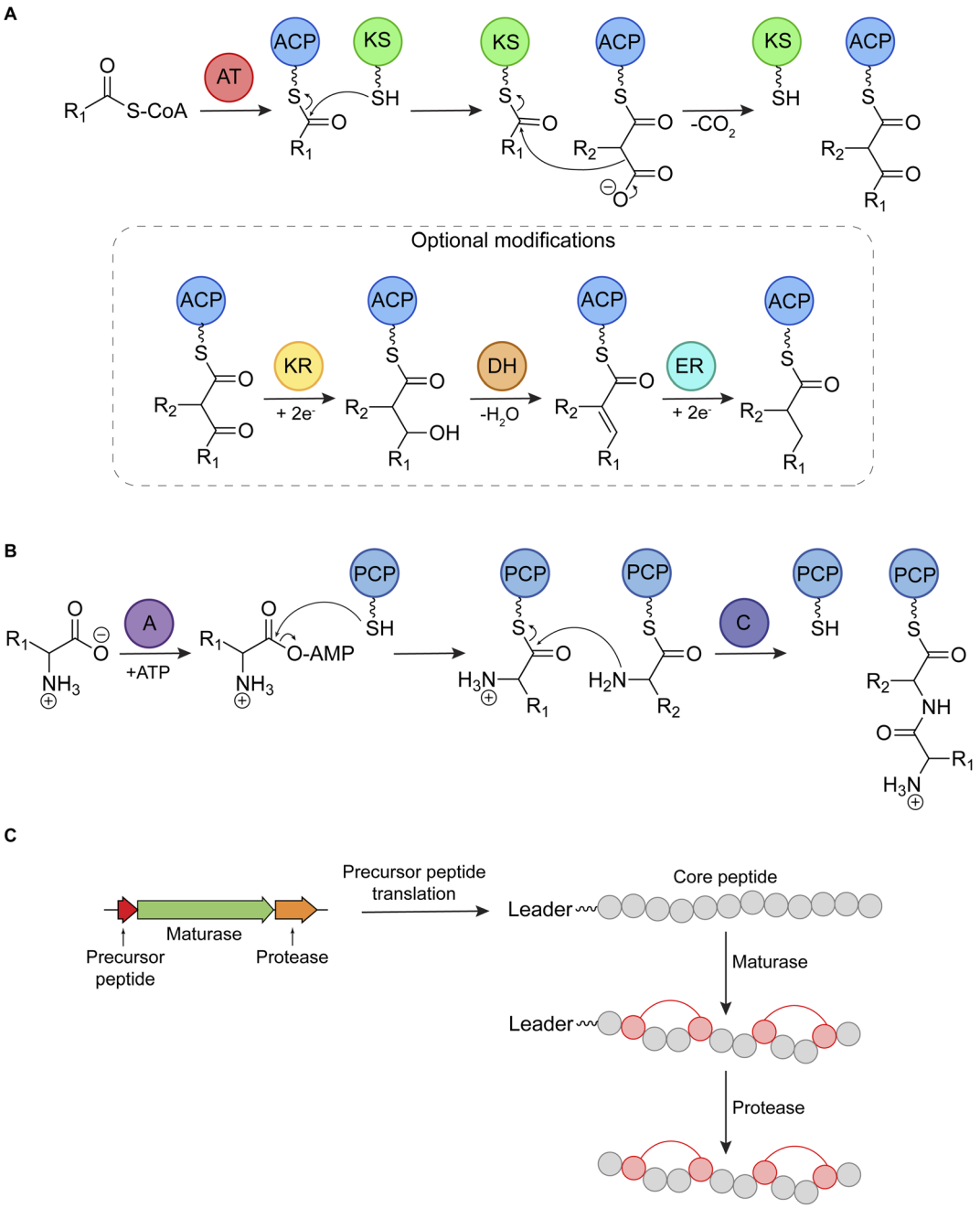

Fig. 1 Principles of polyketide and peptide natural product biosynthesis. (A) Polyketide synthase (PKS) mechanism and optional modifications. AT: acyltransferase, KS: ketosynthase, ACP: acyl carrier protein, KR: ketoreductase, DH: dehydratase, ER: enoylreductase. (B) Non-ribosomal peptide synthetase (NRPS) mechanism. A: adenylation domain, PCP: peptidyl carrier protein, C: condensation domain. (C) Ribosomally synthesized and post-translationally modified peptide (RiPP) biosynthesis.

unlabeled precursors can be fed and their incorporation detected *via* methods such as mass spectrometry (Fig. 2A). This means that any molecule can be used as a precursor, making InverSIL a powerful approach because of its versatility.

InverSIL has also been used extensively in protein NMR spectroscopy studies,[10–13] where it is often referred to as reverse labeling or unlabeling, as well as to track microbial mineralization of dissolved matter.[14] These applications will not be discussed here. In this review, we discuss the advantages and disadvantages of the InverSIL approach and describe cases in which InverSIL has been used to determine biosynthetic routes to natural products. We also discuss applications of InverSIL when the structure of a natural product is not yet known, either to aid structural characterization or to facilitate genome mining by linking biosynthetic gene clusters to their products. Together, these examples highlight the power of the InverSIL approach and its potential for broader adoption by the natural products community.

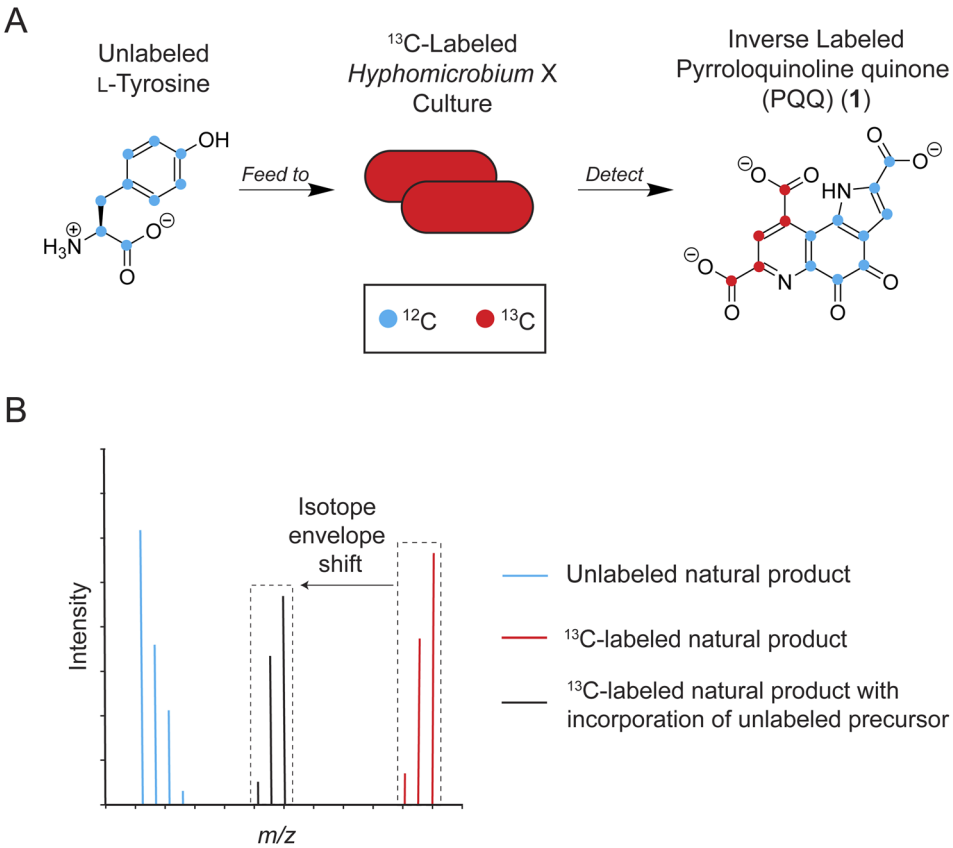

Fig. 2 The InverSIL approach. (A) Identification of L-tyrosine as a precursor of the cofactor pyrroloquinoline quinone (PQQ, **1**) using InverSIL. (B) A mockup of the results of an InverSIL experiment showing three overlaid mass spectra from extracts of three parallel cultures grown with an unlabeled carbon source (blue), a ^{13}C-substituted carbon source (red), and a ^{13}C-substituted carbon source with the addition of an unlabeled precursor (black). The large isotopic envelope shift resulting from inverse labeling of a natural product with an unlabeled precursor containing many ^{12}C atoms is highlighted.

2. Advantages and disadvantages of inverse stable isotopic labeling

Like any method, several factors should be considered when determining whether InverSIL is appropriate for a given natural product study. The most obvious advantage of InverSIL is its ability to circumvent limitations associated with precursor availability. In many cases, an isotopically substituted precursor of interest may be prohibitively expensive, commercially unavailable, or challenging to synthesize. Because InverSIL requires only the nutrient source to be isotopically substituted [for example, with ($^{13}C_6$)glucose], precursors of interest can be fed at their natural isotopic abundance. This feature also enables multiple labeling experiments to be conducted in parallel to screen different potential precursors without the need to purchase or synthesize multiple isotopically substituted compounds.

Additional advantages arise from working with a fully isotopically substituted culture. This approach provides a clear means of distinguishing biologically produced metabolites from abiotic background signals, as metabolites synthesized by the organism become labeled from the isotopically substituted nutrient source.[15,16] Furthermore, because the unlabeled precursors used in InverSIL experiments often contain many of the isotopically distinct atom, particularly in carbon-based InverSIL experiments, the resulting isotopic envelope shifts upon precursor incorporation are relatively large and can be readily detected using automated data analysis methods (Fig. 2B).[17] This property is especially advantageous when InverSIL is applied to the discovery of new natural products that incorporate specific precursors of interest (see section 5).

Despite its utility, InverSIL is not universally suited to all natural product studies. InverSIL is not primarily designed for single-atom tracing; rather, its strengths lie in detecting multi-atom precursor incorporation. Because the method relies on an isotopically substituted background combined with incorporation of an unlabeled precursor, it usually cannot directly label or track a single atom at a specific position within a precursor. This limitation contrasts with traditional stable isotopic labeling approaches, which excel at precise, atom-level mechanistic studies.[18]

Another important consideration is the requirement to generate a fully isotopically labeled culture, which may be difficult or impractical for certain natural product producing organisms including plants and animals. This process is most straightforward when organisms can be grown on chemically defined media, where a single elemental source can be readily replaced with its isotopically substituted counterpart. In

Table 1 Examples of inverse stable isotope labeling used for biosynthetic studies. Legend: (●, ^{12}C) (●, ^{13}C) (●, ^{14}N) (●, ^{15}N)

Stable isotope source (background)	Precursor	Natural product	Ref.
(^{13}C)methanol	L-Tyrosine	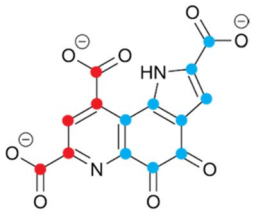 Pyrroloquinoline quinone (PQQ, **1**)	19
ISOGRO-^{13}C	Phenylpyruvate	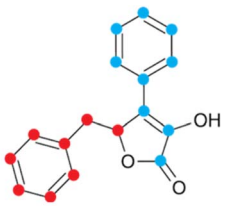 Xenofuranone B (**3**)	22
ISOGRO-^{13}C	Phenylpyruvate[a]	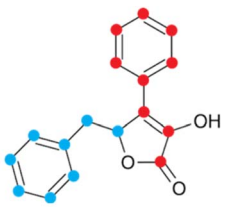 Xenofuranone B (**3**)	22
ISOGRO-^{13}C	L-Leucine	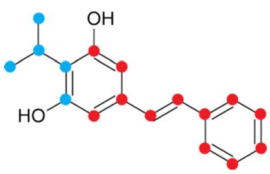 Isopropylstilbene (IPS, **4**)	23
ISOGRO-^{13}C	L-Arginine	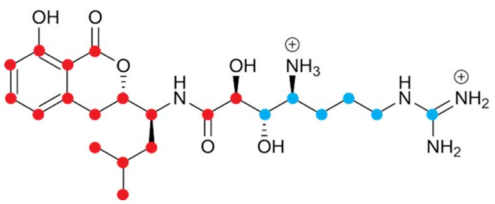 Xenocoumacin I (**5**)	26
ISOGRO-^{13}C	L-Arginine	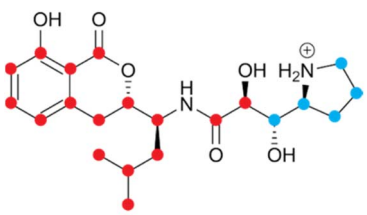 Xenocoumacin II (**6**)	26

Table 1 (*Contd.*)

Stable isotope source (background)	Precursor	Natural product	Ref.
($^{13}C_3$)glycerol	L-Methionine	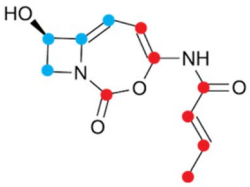 Azetidomonamide A (**8**)	27
($^{13}C_3$)glycerol	L-Serine	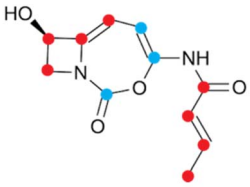 Azetidomonamide A (**8**)	27
($^{13}C_3$)glycerol	L-Methionine	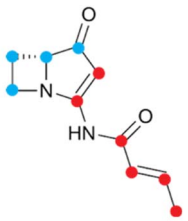 Azetidomonamide B (**9**)	27
($^{13}C_3$)glycerol	L-Serine	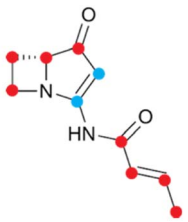 Azetidomonamide B (**9**)	27
($^{13}C_6$)glucose (^{15}N)ammonium chloride	L-Homoserine	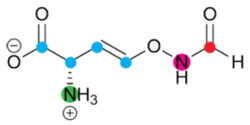 4-Formylaminooxyvinylglycine (FVG, **10**)	29
(^{15}N)ammonium chloride	L-Arginine	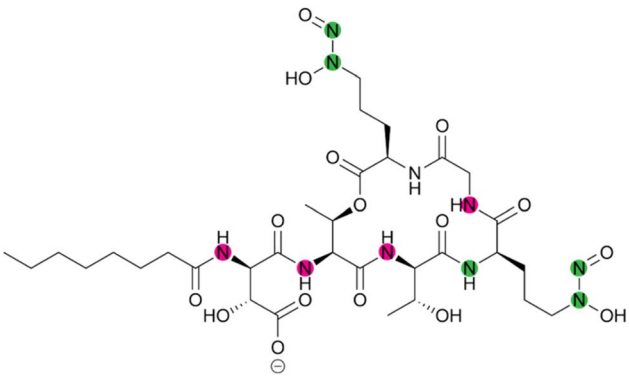 Gramibactin (**13**)	33

Table 1 (*Contd.*)

Stable isotope source (background)	Precursor	Natural product	Ref.
(^{15}N)ammonium chloride	L-Arginine	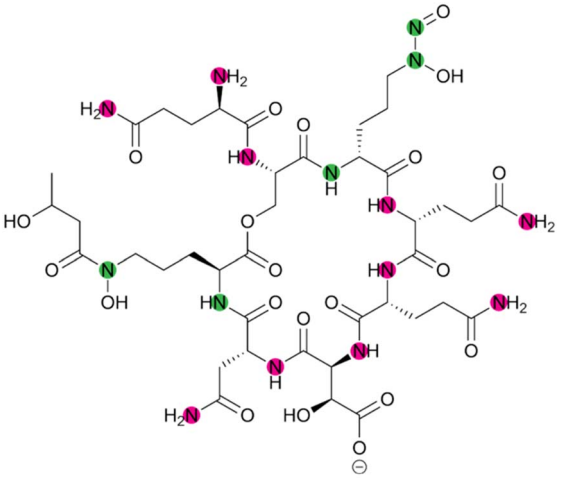 Tistrellabactin A (**14**)	34
($^{13}C_6$)glucose	L-Glutathione	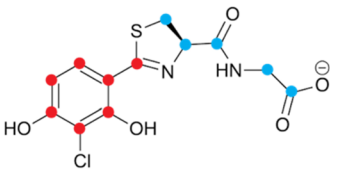 Teredinibactin A (**15**)	35

[a] Phenylpyruvate contributes both a nine-carbon skeleton and a separate eight carbon skeleton to Xenofuranone B.

contrast, organisms that require complex media for growth or natural product production may be less amenable to InverSIL. Although isotopically substituted complex media components are commercially available, their cost may exceed that of a single isotopically labeled precursor. Additionally, because multiple generations of growth are often required to achieve a globally isotopically labeled culture, InverSIL may be impractical on relevant time scales for slow-growing organisms. In some of these cases, including for biosynthetic genes from eukaryotes, heterologous expression in a microbial host capable of growing quickly on a chemically defined medium may provide a viable alternative for access to InverSIL experiments.

Taken together, InverSIL and traditional stable isotopic labeling approaches serve distinct but complementary roles. The choice between these methods should be guided by the specific scientific question, organismal constraints, and practical considerations related to cost and time.

3. Inverse stable isotopic labeling for biosynthetic studies

3.1 Early examples

To our knowledge, the first reported use of InverSIL was to characterize the biosynthesis of the redox-active cofactor

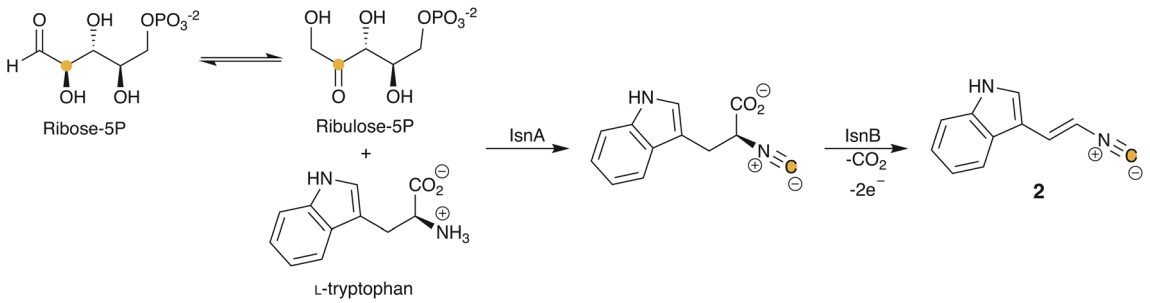

Scheme 1 Origin of the isocyanide carbon (orange circle) in (*E*)-3-(2-isocyanovinyl)-1*H*-indole (**2**).

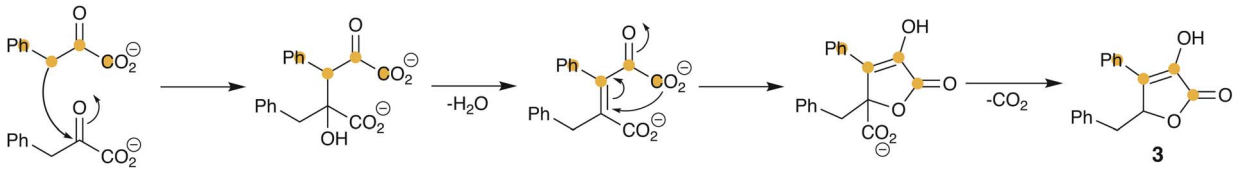

Scheme 2 Proposed biosynthesis of xenofuranone B (3) showing condensation of two phenylpyruvate molecules. Carbons from one phenylpyruvate are distinguished with orange circles.

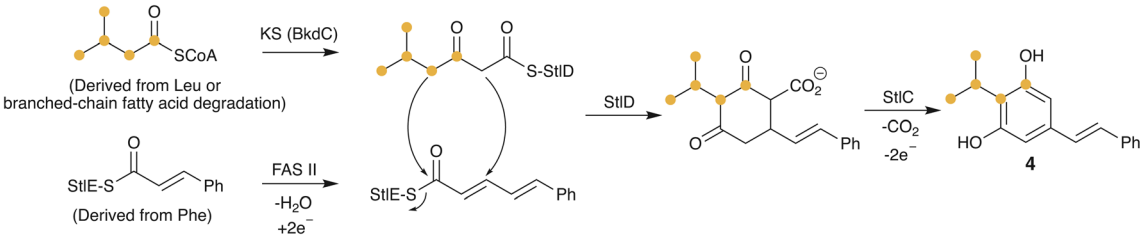

Scheme 3 Biosynthesis of isopropylstilbene (IPS, 4) showing incorporation of a branched chain acyl-CoA (carbons are distinguished with orange circles).

pyrroloquinoline quinone (PQQ, **1**). Van Kleef and Duine (1988)[19] showed that the methanol-utilizing bacterium *Hyphomicrobium* X is capable of uptaking amino acids, and subsequently took advantage of this finding by growing *Hyphomicrobium* X on (^{13}C) methanol and feeding unlabeled L-amino acids to detect incorporation into **1** by gas chromatography-mass spectrometry (GC-MS). This method identified L-tyrosine as a precursor to **1**, which is now known to be a RiPP (Fig. 2A and Table 1). The authors next determined that the *o*-quinone and pyrrole-2-carboxylic acid moieties of PQQ are derived from the complete skeleton of tyrosine by comparing the ^{13}C NMR spectrum of fully substituted ($^{13}C_{14}$)PQQ with the spectrum of a mixture also containing some partially labeled **1** with unlabeled L-tyrosine incorporated. Using InverSIL with methylotrophic bacteria (bacteria that derive all their carbon and energy from reduced carbon substrates lacking C–C bonds) is logical because ^{13}C-substituted one carbon substrates are relatively inexpensive.

Brady and Clardy (2005)[20] used InverSIL to elucidate the biosynthetic origin of the isocyanide group in an antibiotic (**2**) produced by an *E. coli* strain expressing environmental DNA.[21] They grew this strain on ($^{13}C_6$)glucose and unlabeled L-tryptophan, confirming all other carbons in **2** were derived from this amino acid. The authors then grew a series of *E. coli* mutants where specific primary metabolic pathways were blocked on ($^{13}C_6$) glucose to systematically determine the origin of the isocyanide carbon atom by feeding unlabeled sugars as precursors. This series of experiments led them to the pentose phosphate pathway, and subsequent *in vitro* work identified the C2 of ribose-5-phosphate as the origin of the isocyanide carbon (Scheme 1). Because arabinose-5-phosphate was also converted into the antibiotic *in vitro*, the authors proposed that ribulose-5-phosphate is an intermediate in the biosynthesis. Finally, feeding experiments with strains expressing single enzymes in the pathway led the authors to propose that decarboxylation is the final step in the biosynthesis. This study highlights how InverSIL enables rapid screening of many precursors for incorporation into a natural product of interest.

The Bode Group has extensively used InverSIL while studying natural products produced by entomopathogenic bacterial symbionts of nematodes, including for characterizing

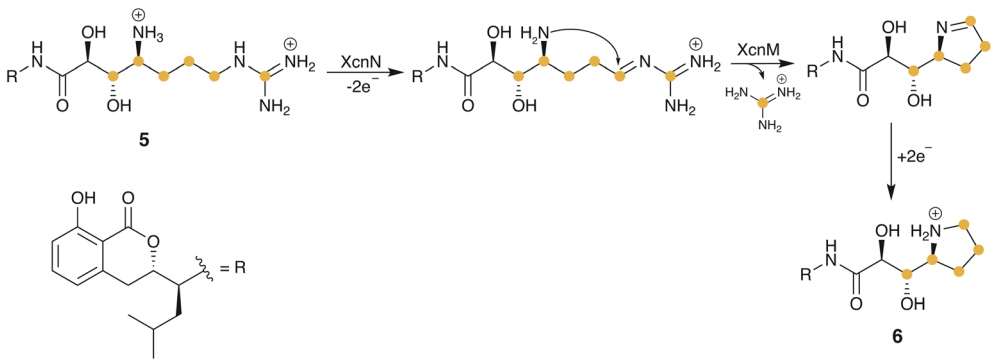

Scheme 4 Proposed biosynthesis of xenocoumacin II (**6**) from xenocoumacin I (**5**). Carbons derived from L-arginine are distinguished with orange circles.

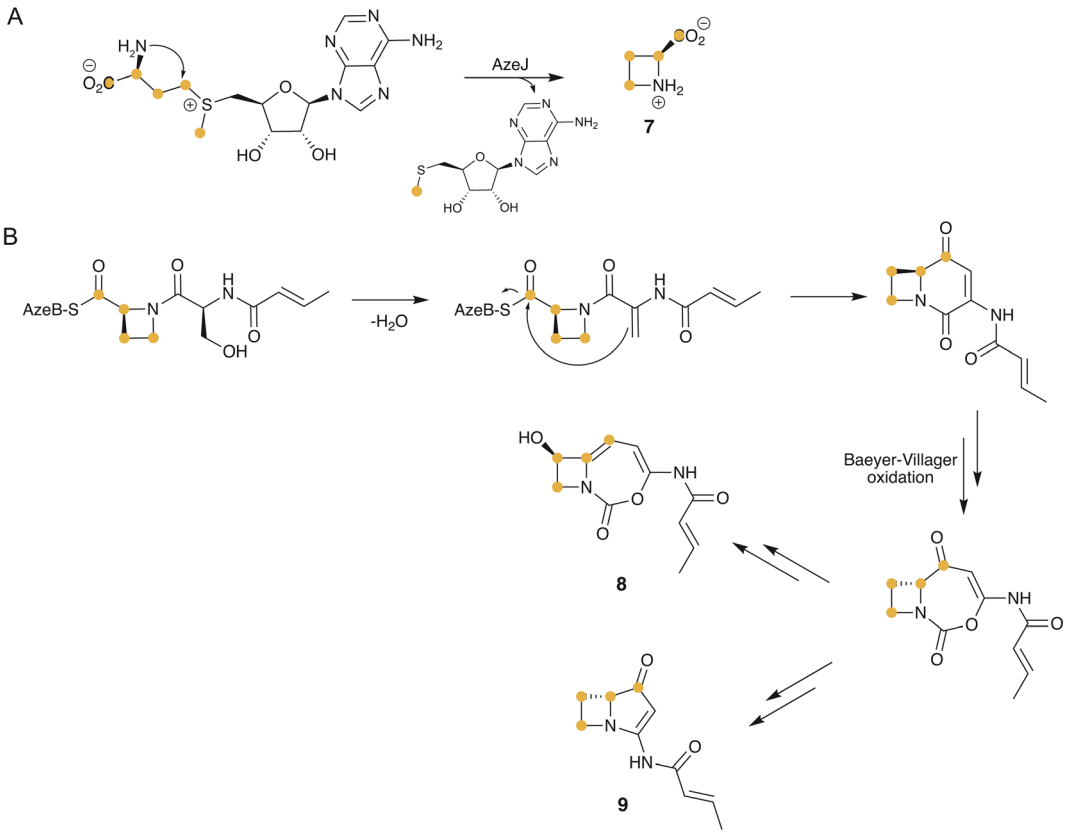

Scheme 5 (A) Formation of azetidine 2-carboxylic acid (AZC, **7**) from *S*-adenosyl-L-methionine. Carbons derived from L-methionine are distinguished with orange circles. (B) Biosynthesis of azetidomonamide A (**8**) and B (**9**). Carbons derived from **7** are distinguished with orange circles.

biosynthetic routes to these compounds. Brachmann *et al.* (2006)[22] used InverSIL to characterize the biosynthesis of the xenofuranones, furanone containing natural products made by the bacterium *Xenorhabdus szentirmaii*. They grew *X. szentirmaii* on the commercially available ^{13}C-substituted complex growth medium ISOGRO-^{13}C and fed the culture unlabeled phenylpyruvate. The authors used GC-MS to observe that one complete nine-carbon skeleton of phenylpyruvate was incorporated into xenofuranone B (**3**), as well as one eight-carbon skeleton. This led them to propose that the furanone ring of these natural products is formed *via* an aldol-type condensation between two phenylpyruvates, followed by cyclization and subsequent decarboxylation (Scheme 2).

Joyce *et al.* (2008)[23] used a similar method with another entomopathogenic bacterium, *Photorhabdus luminescens*, to determine the biosynthesis of isopropylstilbene (IPS, **4**). They used InverSIL to demonstrate that IPS incorporates five carbons from leucine or the branched-chain fatty acid *iso*-15:0. This led the authors to propose that in IPS biosynthesis, one building block is isovaleryl-β-ketoacyl-ACP, derived from the branched-chain α-keto acid dehydrogenase complex (BkdABC). This is then condensed with 5-phenyl-2,4-pentadienoyl-ACP by the

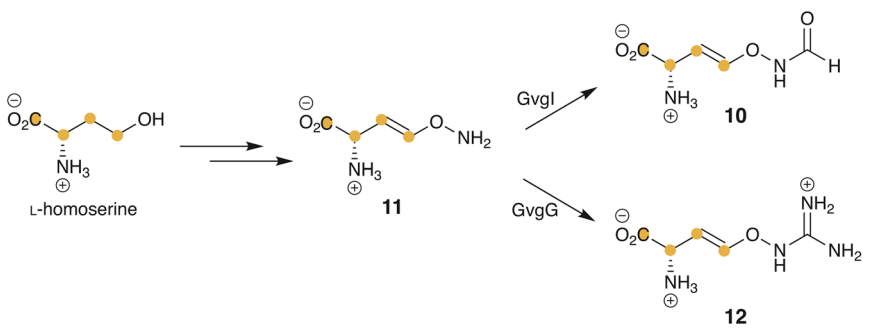

Scheme 6 Biosynthesis of 4-formylaminooxyvinylglycine (**10**), aminooxyvinylglycine (**11**), and guanidinooxyvinylglycine (**12**). Carbons derived from L-homoserine are distinguished with orange circles.

enzyme StlD, and subsequently aromatized by StlC.[24] More recent work has demonstrated that fatty acid synthase II extends cinnamoyl-ACP to create 5-phenyl-2,4-pentadienoyl-ACP, identifying crosstalk between primary and secondary metabolism (Scheme 3).[25]

3.2 Non-proteinogenic amino acids in peptide natural products

InverSIL has proven valuable for elucidating the biosynthetic origins of non-proteinogenic amino acids incorporated into peptide and hybrid natural products, especially in cases where the precursor identity cannot be inferred directly from the final structure. Reimer *et al.* (2009)[26] used InverSIL to determine that L-arginine is the precursor to a polyketide-extended amino acid in the xenocoumacin (XCN I, **5**) family of antibiotics, which are produced by *Xenorhabdus*. In some analogs such as XCN II (**6**), this L-arginine incorporation is not readily apparent due to loss of the guanidinium group and subsequent cyclization to form a pyrrolidine moiety (Table 1). This led the authors to identify a saccharopine dehydrogenase-like enzyme and a desaturase (XcnM and XcnN, respectively) involved in the biosynthesis of the pyrrolidine from L-arginine in XCN II (Scheme 4). Using this logic, they were able to show that **5** is the precursor to **6** and all other XCNs.

Hong *et al.* (2019)[27] used InverSIL to identify the biosynthetic origin of the non-proteinogenic amino acid azetidine 2-carboxylic acid (AZC, **7**) in the azetidomonamide natural products, which are produced by *Pseudomonas aeruginosa*. The authors grew *P. aeruginosa* on ($^{13}C_3$)glycerol and fed unlabeled L-methionine as a precursor, which was incorporated into the azetidine moiety of azetidomonamide A (**8**) as well as azetidomonamide B (**9**), which is also called azabicyclene.[28] **7** is formed from *S*-adenosylmethionine (SAM) in plants, and the incorporation of L-methionine was consistent with the presence of a similar biosynthetic route in *P. aeruginosa*. This led to the discovery that AzeJ, a SAM-utilizing enzyme encoded in the bacterium's genome, is an AZC synthase (Scheme 5A). Furthermore, the authors used InverSIL to determine that serine is also a precursor to both azetidomonamides, leading them to propose that the serine-containing precursor peptide is dehydrated and subsequently cyclizes en route to these natural products (Scheme 5B).

Lescallette *et al.* (2022)[29] characterized the biosynthesis of the antibacterial and herbicidal non-proteinogenic amino acid 4-formylaminooxyvinylglycine (FVG, **10**), which is produced by several *Pseudomonas fluorescens* strains. **10** is an oxyvinylglycine, which is a member of a small group of non-proteinogenic amino acids containing a vinyl oxygen moiety, which also includes the antifungals aminooxyvinylglycine (AOVG, **11**) and guanidinooxyvinylglycine (GOVG, **12**). The authors used InverSIL to determine that these amino acids derive from L-homoserine. By growing *P. fluorescens* with ($^{13}C_6$)glucose as the sole carbon source and (^{15}N)ammonium chloride as the sole nitrogen source and subsequently feeding the culture unlabeled L-homoserine, the authors deduced that the carbon backbone and α-amino group are derived from homoserine. Heterologous expression and gene deletion experiments led the authors to propose that in *P. fluorescens* **11** is the common precursor of both **10** and **12**, and the formyltransferase GvgI then converts **11** to **10**, while the amidinotransferase GvgD converts **11** to **12** (Scheme 6). They showed that GvgI is indeed a formyltransferase, while subsequent work has shown that GvgD is

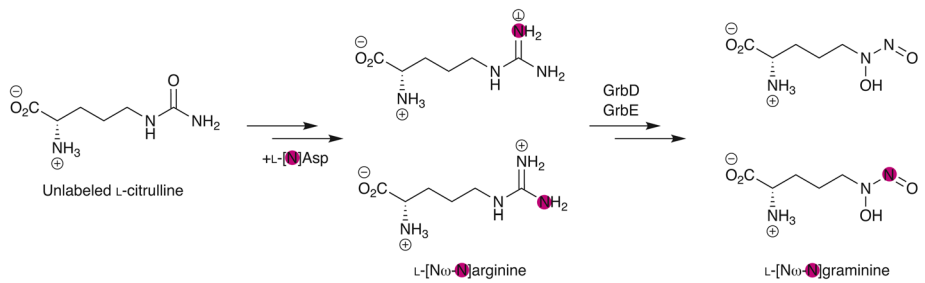

Scheme 7 Determination of the source of the N–N bond in the graminine diazendiumdiolate group. ^{15}N atoms are distinguished with pink circles.

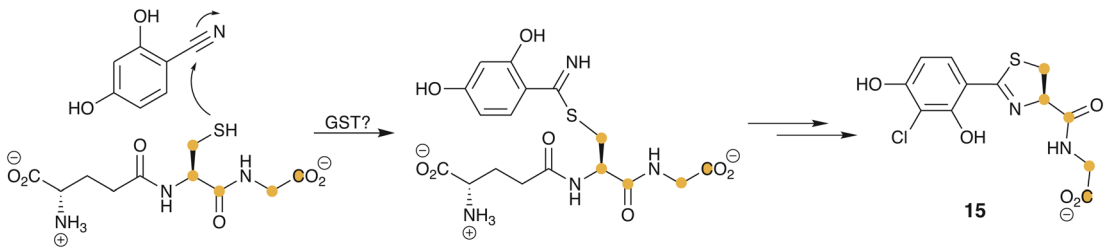

Scheme 8 Proposed biosynthesis of teredinibactin A (**15**). Carbons derived from CysGly are distinguished with orange circles. GST: glutathione-*S*-transferase.

an amidinotransferase.[30] However, it is still possible that **11** is created *via* hydrolysis of **10** and/or **12**.[31]

3.3 Metallophores

Metals are an essential nutrient for nearly all forms of life, and microorganisms often use natural products called metallophores to access metals in their environments. Metallophores often contain atypical, frequently non-proteinogenic amino acids important for chelating different metals.[32] InverSIL provides a powerful approach for determining the origins of these distinctive structural features.

Makris *et al.* (2022)[33] used InverSIL to determine the biosynthetic route to the non-proteinogenic amino acid L-graminine in the siderophore (iron-binding metallophore) gramibactin (**13**) produced by *Paraburkholderia graminis* (Table 1). Graminine has a characteristic C-type diazeniumdiolate group, and the origin of this new Fe(III) coordination ligand was unknown. To investigate the origin of graminine, the authors used an InverSIL approach focused on the origin of the graminine nitrogens. They grew *P. graminis* with (^{15}N)ammonium chloride as the sole nitrogen source, and fed unlabeled L-arginine which led to incorporation of four N atoms into graminine. By feeding unlabeled L-citrulline, a precursor to L-arginine, the authors were able to determine that the N–N in the diazeniumdiolate group is formed from the Nδ and one Nω of the guanidinium group of L-arginine (Scheme 7). More recently, Makris *et al.* (2023)[34] used a similar approach to confirm that the L-graminine residues from a newly characterized group of siderophores, the tistrellabactins (**14**), also originate from L-arginine.

Sung *et al.* (2025)[35] characterized the non-canonical origin of a thiazoline moiety in the metallophore teredinibactin (**15**). They hypothesized that **15** belongs to a class of natural products called glutathione-derived azol(in)es or glutazolines. To prove this, they cultivated the shipworm symbiont, *Teredinibacter turnerae* T7901, using ($^{13}C_6$)glucose and/or (^{15}N)ammonium chloride as the sole carbon/nitrogen source and fed the culture unlabeled glutathione and its metabolic product, Cys–Gly, in separate experiments. The InverSIL data showed the same number of carbon/nitrogen incorporations from glutathione and Cys–Gly in the thiazoline moiety of **15**, indicating that the thiazoline contains the carbon backbone of glutathione-derived Cys–Gly. One possible biosynthetic route to this metallophore proposed by the authors involves the glutathione-*S*-transferase (GST)-catalyzed addition of glutathione to an electrophilic resorcinol derivative, followed by thiazoline formation (Scheme 8).

4. Inverse stable isotopic labeling for natural product structural elucidation

Natural products are often produced in very small amounts, which can impede researchers' ability to elucidate their structures using less sensitive methods such as NMR spectroscopy. High-resolution tandem mass spectrometry is a complementary tool for structural elucidation that is very sensitive, although it does not provide the same connectivity information as NMR spectroscopy. Stable isotopic labeling experiments, including InverSIL, that are analyzed by mass spectrometry can confirm the building blocks of natural products including those present in crude extracts at low concentrations without the need for purification, thereby aiding in the structural elucidation of these compounds. Our criteria for determining if InverSIL was used for structural elucidation or biosynthetic studies was asking if the structure of the natural product was confirmed before the InverSIL experiment was performed. If not, InverSIL contributed to the structural elucidation although it could still provide biosynthetic information as well.

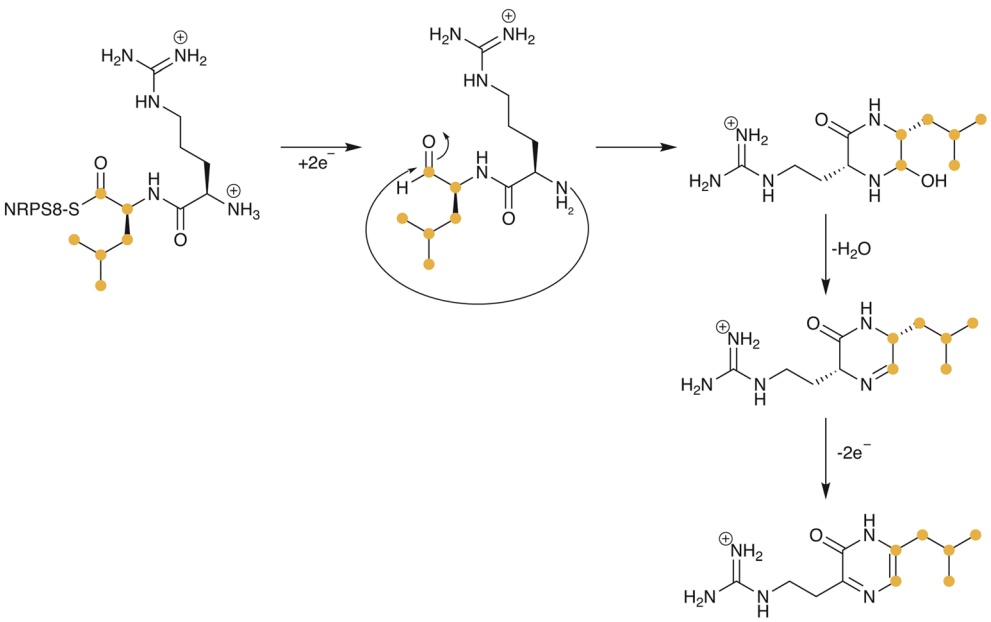

Scheme 9 Pyrazinone biosynthesis by an engineered NRPS. Carbons derived from L-leucine are distinguished with orange circles.

4.1 Non-ribosomal peptides containing proteinogenic amino acids

Stable isotopic labeling for building block determination is an especially powerful approach for peptidic natural products such as NRPs and RiPPs. While tandem mass spectrometry alone can often determine the amino acid composition and sequence of peptidic natural products, combining tandem mass spectrometry with isotopic labeling can accelerate the structural elucidation of modified or non-proteinogenic peptide sequences and differentiate between isobaric amino acids (*e.g.* leucine and isoleucine). The Bode Group pioneered the use of InverSIL for natural product building block determination, again with a focus on natural products made by entomopathogenic bacteria. In an early example, Fuchs *et al.* (2011)[36] used

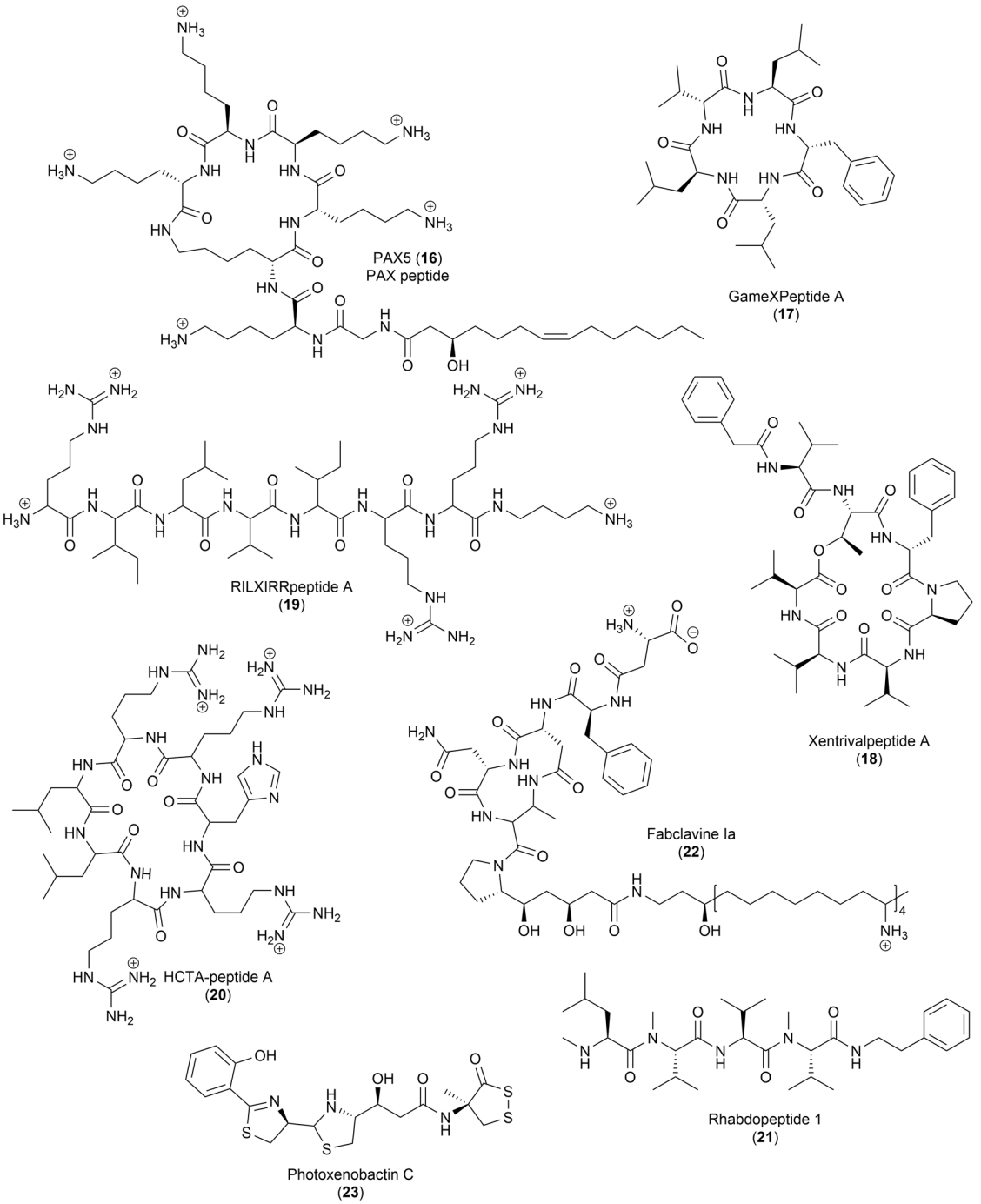

InverSIL during their rigorous characterization of the structures of thirteen new PAX (peptide-antimicrobial-*Xenorhabdus*) peptides (**16**). They grew *Xenorhabdus nematophila* on the ^{13}C-substituted complex growth medium ISOGRO-^{13}C and detected incorporation of unlabeled L-arginine and L-lysine residues into various PAX peptides (**16**). By combining this approach with other mass spectrometry-based methods such as derivatization, the authors were able to characterize some NRPs without the need for purification, demonstrating the power of combining InverSIL and mass spectrometry.

In addition to **16**, the Bode Group has used InverSIL to identify the amino acid building blocks of other NRPS products including the GameXPeptides (**17**),[37] the xentrivalpeptides (**18**),[38] the RILXIRRpeptides (**19**, stereochemistry not reported),[39] the HCTA-peptides (**20**, stereochemistry not reported),[39] the rhabdopeptides (**21**),[40] and the fabclavines (**22**).[41] They also used InverSIL to help identify a unique dithioperoxoate moiety composed of cysteine in photoxenobactin C (**23**).[42]

The affordability of genome sequencing and the development of natural product-focused bioinformatic tools has led to modern natural product structural elucidation often being guided by the analysis of biosynthetic gene clusters (BGCs). For NRPSs, adenylation domain prediction has proven helpful for targeted labeling of peptidic natural products, including when these BGCs are heterologously expressed. InverSIL helped elucidate the structures of the products of heterologously expressed NPRSs in yeast or *E. coli* including ambactin (**24**),[43] the luminmides (**25**)[44] (which are the same natural product family as the GameXPeptides), and the ririwpeptides (**26**).[45] It also helped to identify an unnatural pyrazinone moiety in a natural product formed by an engineered NRPS containing an aldehyde-forming terminal reductase domain (Scheme 9).[46]

4.2 Non-ribosomal peptides containing non-proteinogenic amino acids and other precursors

Researchers have used InverSIL to help elucidate the structures of natural products that incorporate building blocks other than proteinogenic amino acids. The *C*-terminal residues of bicornutin A1 (**27**) and A2 (**28**) were determined by feeding the amines putrescine and phenylethylamine, respectively.[39] In the siderophore, fimsbactin (**29**), the catechol moiety 2,3-dihydroxybenzoic acid and the amine 1,4-diaminopropane were fed to help elucidate the structures of multiple analogs of this siderophore.[47] In xenoamicin (**30**), feeding with beta-alanine confirmed the presence of a beta amino acid.[48] In photoditritide (**31**) InverSIL identified the presence of a rare homoarginine residue in its structure.[49] Lastly, in taxlllaid, branched-chain fatty acids (*iso*-7:0 (**32**), *iso*-5:0 (**33**), *iso*-4:0 (**34**)) were fed to determine *N*-terminal acyl groups.[50] Some of these precursors are not commercially available in an isotopically labeled form or are prohibitively expensive, again showing the power of the InverSIL approach.

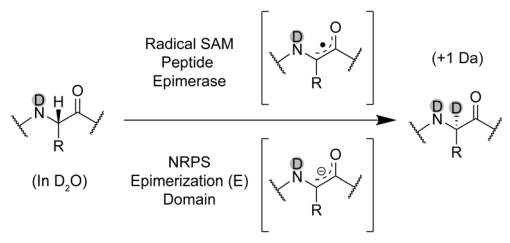

Fig. 3 Detection of epimerization modifications in peptide natural products using InverSIL.

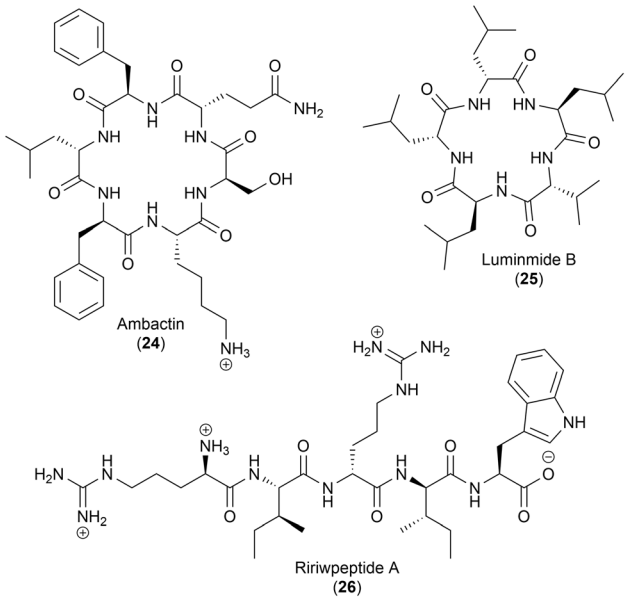

4.3 Determining stereochemistry of peptidic natural products

A different version of InverSIL can be used to determine the absolute configuration of amino acids in peptide natural products. Peptidic natural products can contain L- and/or D-amino acids, and NRPSs can convert incorporated L-amino acids into D-amino acids through epimerization (*E*) domains that abstract the amino acid's α-proton, which is then replaced by an exchangeable proton to invert the stereochemistry at this position (Fig. 3).[51] Bode *et al.* (2012)[37] demonstrated that by feeding producing organisms deuterated amino acids, researchers can detect epimerization by mass spectrometry by identifying the loss of the α-deuterium and its replacement with a hydrogen, which leads to a −1 Da mass shift for each D-amino acid. Because some α-deuterated amino acids can be expensive or unavailable, Kegler *et al.* (2014)[52] developed an inverse version of this method in which the producing strain is grown in D_2O and fed nondeuterated amino acids. In this case, epimerization results in a mass shift of +1 Da for each D-amino acid (Fig. 3). The authors used this method to confirm the absolute configuration of the new NRP xenotetrapeptide when its BGC was heterologously expressed in *E. coli*. It should be noted that for this strategy to work, it must be performed in a strain where the host transaminases have been deleted so that these enzymes do not remove the label from the amino acid precursor.[37,52] RiPPs can also contain D-amino acids, which are installed post-

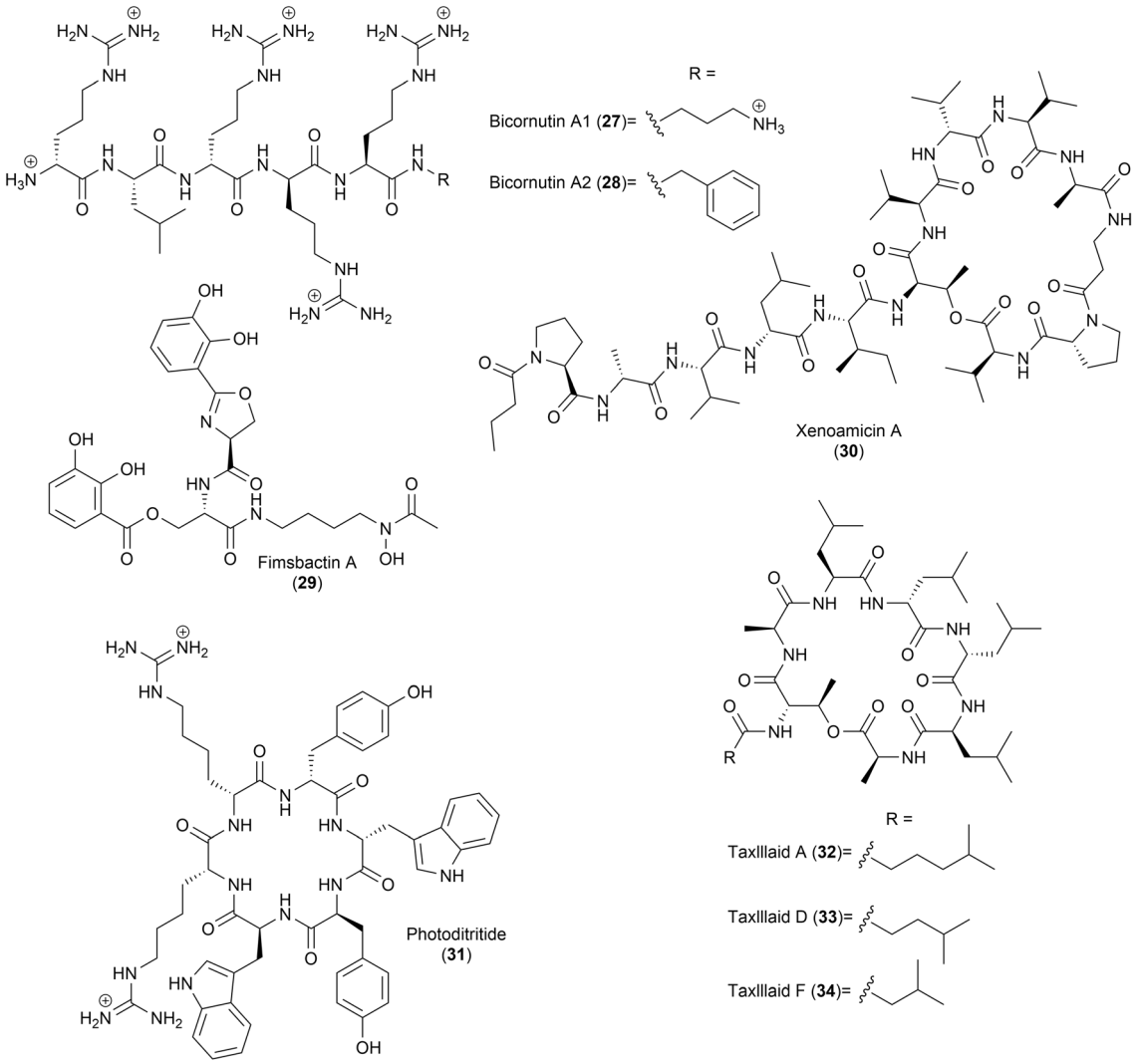

translationally by radical-SAM epimerases.[53,54] Morinaka *et al.* (2017)[55,56] developed an orthogonal D_2O based induction system (ODIS) analogous to the NRPS system to assign the absolute stereochemistry of RiPPs (Fig. 3). They used this method to help decipher some of the chemical logic behind the regioselectivity of radical-SAM epimerases.

4.4 Polyketides

In a different application of InverSIL, Li *et al.* (2023)[57] characterized the products of animal fatty acid synthase-like polyketide synthases (AF-PKSs), an unexplored family of phylogenetically widespread enzymes in eukaryotes. Through heterologous expression and *in vitro* enzyme assays, they showed that these AF-PKS enzymes can produce a diverse set of pyrone polypropionate natural products, which could be attributed to the enzyme's starter unit promiscuity. They used a wide range of unlabeled starter units in reactions with ($^{13}C_4$) methylmalonyl-CoA as the extender unit, which enabled them to identify multiple products with different starter unit incorporation (Scheme 10). In their experiments, some products were found to be in low abundance or were less stable, and thus InverSIL and mass spectrometry were key to their structural assignments.

5. Inverse stable isotopic labeling for genome mining-based natural product discovery

Stable isotopic labeling has also been used to discover natural products that incorporate precursors of interest. When precursors are chosen based on the presence of specific biosynthetic genes in an organism's genome, this has been referred to as the genomisotopic approach.[58] In cyanobacteria, this approach has

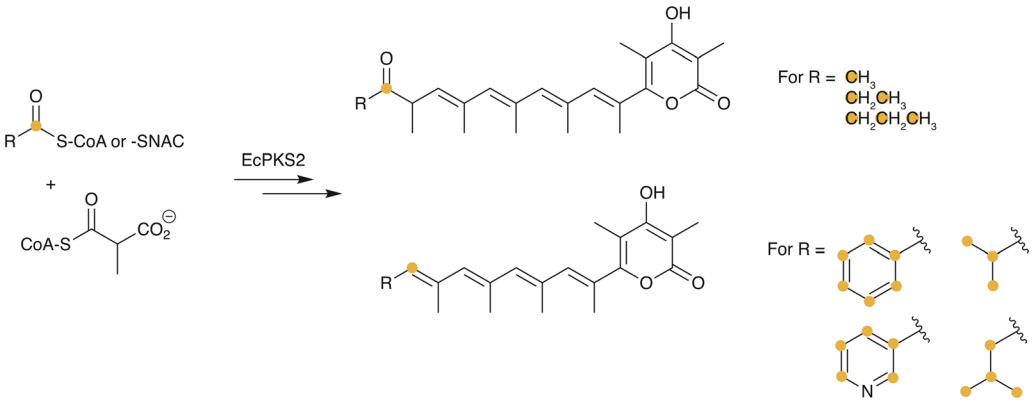

Scheme 10 Starter unit promiscuity of EcPKS2 to produce various polypropionates. Starter unit-derived carbons are distinguished with orange circles.

been used to link NRPS BGCs[59,60] and BGCs encoding for fatty acid containing compounds[61] with their products. The Linington Group has generalized this approach with a systematic isotope-feeding platform for linking natural products with BGCs termed IsoAnalyst.[62] This approach predicts how many generalist precursors such as (1-^{13}C)acetate and (1-^{15}N)glutamate are likely incorporated into a BGC of interest, and has been used to identify the products of several BGCs.[63,64] Here we focus on how InverSIL can also be used to enhance genome mining by linking biosynthetic genes with their natural products (Fig. 4A).[65]

5.1 Quorum sensing signals

Quorum sensing signals are natural products that bacteria use to coordinate group behaviors.[66,67] Cummings *et al.* (2021)[68] used InverSIL to identify the quorum sensing signal products of *N*-acyl-homoserine lactone (acyl-HSL) synthases encoded in the genomes of methylotrophic bacteria that grow on methanol, methylamine, or methane gas. In this work they grew the bacteria on ^{13}C-substituted versions of these carbon sources, which are relatively inexpensive, and then fed the cultures unlabeled L-methionine, which forms the HSL core of these

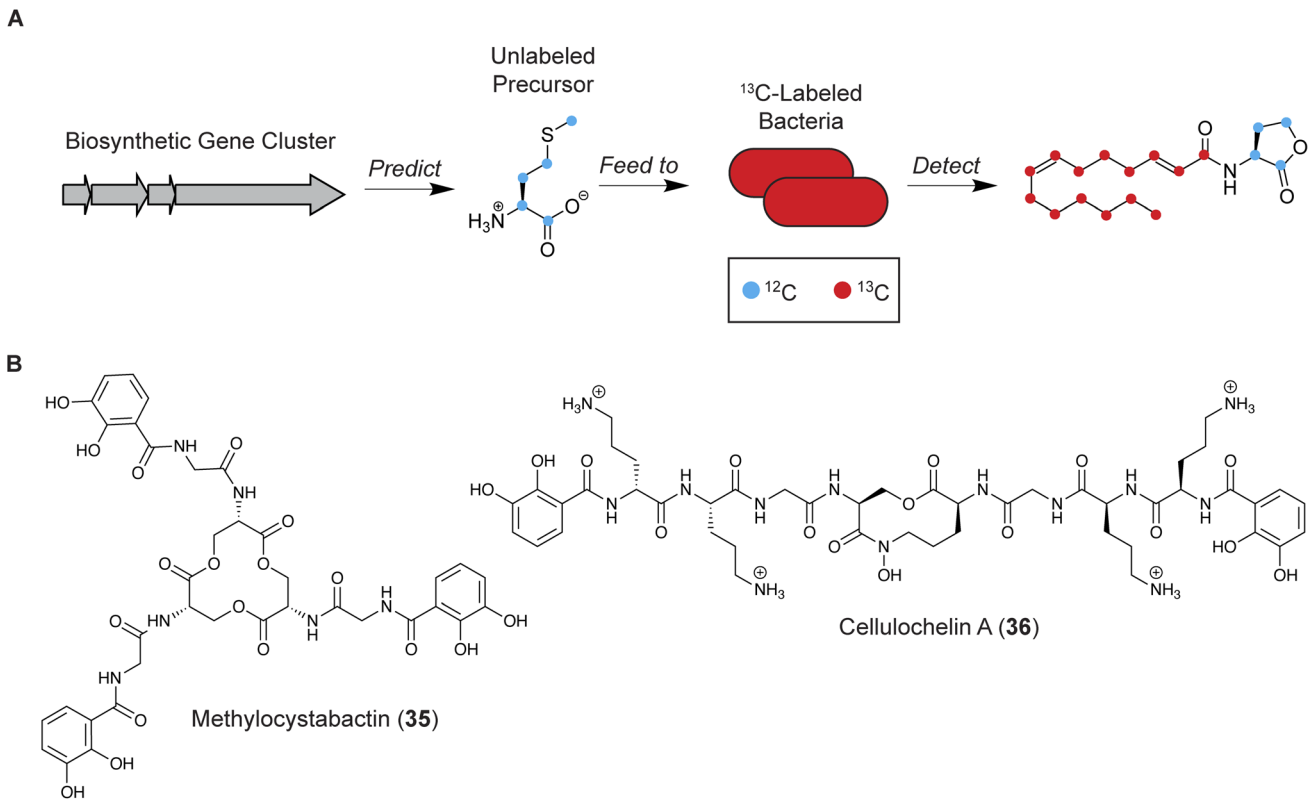

Fig. 4 Using InverSIL to link biosynthetic gene clusters (BGCs) with their natural products. (A) An example of this approach demonstrating how unlabeled L-methionine is used to discover the quorum sensing signal product of an acyl-homoserine lactone synthase. (B) Catecholate siderophores that have been linked to their BGCs using the InverSIL approach with unlabeled 2,3-dihydroxybenzoic acid (2,3-DHB).

signals *via* SAM (Fig. 4A). Guided by genomic information, they used this method to identify five uncharacterized acyl-HSL quorum sensing signals produced by the methanol-utilizer *Methylorubrum rhodinum* and to link these signals with the synthases that produce them. To avoid manually inspecting each culture condition for precursor incorporation, they used automated analysis of mass spectral features to identify pairs of features with matching retention times and a mass downshift of 4 Da in the inverse labeled condition, indicating L-methionine incorporation into the HSL core. Wallace *et al.* (2023)[69] used the same approach to identify an acyl-HSL with a new structure that is produced by the largest family of acyl-HSL synthase enzymes in the genomes of pink-pigmented facultative methylotrophs, an ecologically important group bacteria.

5.2 Catecholate siderophores

Catecholate siderophores are defined by the presence of catecholate hydroxyl groups derived from 2,3- or 3,4-dihydroxybenzoic acid (DHB), which confer some of the highest known affinities for iron(III) by coordinating the metal through bidentate interactions.[70,71] The biosynthesis of DHB moieties can be predicted in bacterial genomes, which is an effective way to identify BGCs that may produce catecholate siderophores. Robes *et al.* (2025)[72] introduced and applied a variant of InverSIL called inverse stable isotope probing-metabolomics (InverSIP) to link a highly transcribed BGC in a complex methane-oxidizing bacterial community with its catecholate siderophore product. The BGC was identified using a combination of metagenomics and metatranscriptomics, and it was linked to its catecholate siderophore product by growing the methane-oxidizing bacterial community on (^{13}C)methane with unlabeled 2,3-DHB added. Once the inverse labeled metabolite was discovered, MS2 fragmentation and purification from an isolated strain led to the discovery of methylocystabactin (**35**) (Fig. 4B), a widespread triscatecholate siderophore in methanotrophic alphaproteobacteria in the family Methylocystaceae.

Building on this work, the same research group recently applied InverSIL to link predicted catecholate BGCs with their siderophore products across diverse bacterial taxa.[73] This approach was successfully applied to siderophores constructed by both NRPS-dependent and NRPS-independent pathways. Using InverSIL, they characterized two siderophores involved in *Chromobacterium violaceum* virulence that had not previously been structurally characterized. InverSIL also revealed cryptic enterobactin BGCs where the biosynthetic genes are distributed across the genome, obscuring genomic-based prediction of biosynthetic potential. Lastly, the authors used InverSIL to identify and characterize previously undescribed siderophores, cellulochelin A (**36**) (Fig. 4B) and cellulochelin B, produced by a *Cellulomonas* species associated with plants.

At the time of these studies, 2,3-DHB was not readily commercially available in an isotopically labeled form, highlighting the important role of InverSIL in this work. By combining genomic prediction with InverSIL, this approach highlights the versatility of this approach for connecting predicted BGCs with their products. More broadly, it shows the power of using InverSIL in a functional group-directed manner, which may be extended to other natural products with distinct structural features of interest.

6. Conclusion

The versatility of InverSIL expands the already significant power of stable isotopic labeling for natural product characterization and discovery. InverSIL complements traditional isotopic labeling experiments and may be the first choice in cases where an isotopically substituted precursor is unavailable, and/or many precursors need to be screened in parallel. Although still limited in examples compared to traditional isotopic labeling approaches in the natural product field, the power of InverSIL has been demonstrated by researchers for characterizing the biosynthetic routes to natural products, determining the structures of these compounds, and linking BGCs of interest to new natural products.

7. Future outlook

In the future, InverSIL has the potential to accelerate the discovery of additional natural products that contain precursors of interest, including by rapidly linking these compounds to their BGCs. For example, InverSIL could be used more systematically similar to IsoAnalyst,[62] by linking natural products to their BGCs using homology-based structural prediction and the incorporation patterns of labeled precursors. InverSIL could expand the number of BGC types applicable to this approach by enabling access to a more diverse group of isotopically distinct precursors.

InverSIL has proven to be a powerful tool for natural product structural elucidation (section 4). More generally, combining isotopic labeling with molecular networking approaches[74] has the potential to annotate more metabolomic "dark matter," including through the identification of more derivatives of existing natural products. The use of InverSIL approaches with purified enzymes can likely also be further expanded. For example, this approach may be useful for rapidly characterizing the products of engineered biocatalysts.

Although current examples have focused primarily on bacteria, InverSIL should also be applicable to other microorganisms capable of growth on chemically defined media, such as fungi and microalgae. These organisms possess biosynthetic pathways and produce compounds distinct from bacteria. For example, the cytochalasans[75] are a family of fungal natural products that obtain their structural diversity from both the incorporation of different amino acids as well as decoration with unique functional groups installed by various enzymes. This provides exciting opportunities for labeling studies. Beyond pure cultures, InverSIL could also be used to track the modification of unlabeled natural products by neighboring strains in microbial communities, which would enable a greater understanding of the chemical ecology of these consortia.

In the case of plant and animal natural products, creating ^{13}C-labeled host organisms is challenging, limiting access to the InverSIL approach. Heterologous expression of biosynthetic pathways of interest is one way to circumvent this issue, and expression of these pathways in organisms that grow on

inexpensive feedstocks such as methanol may make this a more economical venture. In some cases, isotopic labeling can also be applied directly to animals. For example, researchers achieved *in vivo* isotopic labeling of polypropionates produced by photosynthetic mollusks by injecting [1-^{13}C]-propionate.[76] Similar to the *in vitro* application used in section 4.4, InverSIL may be useful to identify other mollusk-derived polypropionates with unique starter and/or extender units.

Together, these possibilities position InverSIL as a versatile platform for expanding both natural product discovery and our understanding of microbial metabolism and interactions.

8. Conflicts of interest

The authors declare no conflicts of interest.

9. Data availability

No primary research results, software or code have been included and no new data were generated or analysed as part of this review.

10. Acknowledgements

This work was supported by the National Institute of General Medical Sciences of the National Institutes of Health under award number R35 GM147018 (to A.W.P.). The content is solely the responsibility of the authors and does not necessarily represent the official views of the National Institutes of Health.

11. References

1 D. J. Newman and G. M. Cragg, *J. Nat. Prod.*, 2020, **83**, 770–803.
2 T. A. Scott and J. Piel, *Nat. Rev. Chem.*, 2019, **3**, 404–425.
3 U. T. Bornscheuer, G. W. Huisman, R. J. Kazlauskas, S. Lutz, J. C. Moore and K. Robins, *Nature*, 2012, **485**, 185–194.
4 A. Hou and J. S. Dickschat, *Nat. Prod. Rep.*, 2023, **40**, 470–499.
5 J. Rinkel and J. S. Dickschat, *Beilstein J. Org. Chem.*, 2015, **11**, 2493–2508.
6 International Union of Pure and Applied Chemistry, in *Nomenclature of Organic Chemistry: IUPAC Recommendations and Preferred Names 2013*, ed. H. A. Favre and W. H. Powell, Royal Society of Chemistry, Cambridge, UK, 2013.
7 A. Nivina, K. P. Yuet, J. Hsu and C. Khosla, *Chem. Rev.*, 2019, **119**, 12524–12547.
8 R. D. Süssmuth and A. Mainz, *Angew. Chem., Int. Ed.*, 2017, **56**, 3770–3821.
9 M. Montalbán-López, T. A. Scott, S. Ramesh, I. R. Rahman, A. J. Van Heel, J. H. Viel, V. Bandarian, E. Dittmann, O. Genilloud, Y. Goto, M. J. Grande Burgos, C. Hill, S. Kim, J. Koehnke, J. A. Latham, A. J. Link, B. Martínez, S. K. Nair, Y. Nicolet, S. Rebuffat, H.-G. Sahl, D. Sareen, E. W. Schmidt, L. Schmitt, K. Severinov, R. D. Süssmuth, A. W. Truman, H. Wang, J.-K. Weng, G. P. Van Wezel, Q. Zhang, J. Zhong, J. Piel, D. A. Mitchell, O. P. Kuipers and W. A. Van Der Donk, *Nat. Prod. Rep.*, 2021, **38**, 130–239.
10 P. Brodin, T. Drakenberg, E. Thulin, S. Forsén and T. Grundström, *Protein Eng. Des. Sel.*, 1989, **2**, 353–357.
11 D. Shortle, *J. Magn. Reson. B*, 1994, **105**, 88–90.
12 G. W. Vuister, S.-J. Kim, C. Wu and A. Bax, *J. Am. Chem. Soc.*, 1994, **116**, 9206–9210.
13 D. Lacabanne, B. H. Meier and A. Böckmann, *J. Biomol. NMR*, 2018, **71**, 141–150.
14 X. Dong, M. A. Jochmann, M. Elsner, A. H. Meyer, L. E. Bäcker, M. Rahmatullah, D. Schunk, G. Lens and R. U. Meckenstock, *Environ. Sci. Technol.*, 2017, **51**, 11876–11883.
15 N. G. Mahieu, X. Huang, Y.-J. Chen and G. J. Patti, *Anal. Chem.*, 2014, **86**, 9583–9589.
16 A. C. Mosier, N. B. Justice, B. P. Bowen, R. Baran, B. C. Thomas, T. R. Northen and J. F. Banfield, *mBio*, 2013, **4**, 00484.
17 T. C. E. Liebergesell, E. G. Murdock and A. W. Puri, *Anal. Chem.*, 2024, **96**, 16330–16337.
18 A. Hou and J. S. Dickschat, *Nat. Prod. Rep.*, 2023, **40**, 470–499.
19 M. A. van Kleef and J. A. Duine, *FEBS Lett.*, 1988, **237**, 91–97.
20 S. F. Brady and J. Clardy, *Angew. Chem., Int. Ed.*, 2005, **44**, 7045–7048.
21 S. F. Brady and J. Clardy, *Angew. Chem.*, 2005, **117**, 7225–7227.
22 A. O. Brachmann, S. Forst, G. M. Furgani, A. Fodor and H. B. Bode, *J. Nat. Prod.*, 2006, **69**, 1830–1832.
23 S. A. Joyce, A. O. Brachmann, I. Glazer, L. Lango, G. Schwär, D. J. Clarke and H. B. Bode, *Angew. Chem., Int. Ed.*, 2008, **47**, 1942–1945.
24 T. Mori, T. Awakawa, K. Shimomura, Y. Saito, D. Yang, H. Morita and I. Abe, *Cell Chem. Biol.*, 2016, **23**, 1468–1479.
25 S. Kavakli, G. L. C. Grammbitter and H. B. Bode, *Tetrahedron*, 2022, **128**, 133116.
26 D. Reimer, E. Luxenburger, A. O. Brachmann and H. B. Bode, *ChemBioChem*, 2009, **10**, 1997–2001.
27 Z. Hong, A. Bolard, C. Giraud, S. Prévost, G. Genta-Jouve, C. Deregnaucourt, S. Häussler, K. Jeannot and Y. Li, *Angew. Chem., Int. Ed.*, 2019, **58**, 3178–3182.
28 J. B. Patteson, A. R. Lescallette and B. Li, *Org. Lett.*, 2019, **21**, 4955–4959.
29 A. R. Lescallette, Z. D. Dunn, V. A. Manning, K. M. Trippe and B. Li, *Biochemistry*, 2022, **61**, 2159–2164.
30 L. Pang, W. Niu, Y. Duan, X. Bian, Y. Zhang and G. Zhong, *Org. Chem. Front.*, 2023, **10**, 2782–2789.
31 A. R. Lescallette, Z. D. Dunn, V. A. Manning, K. M. Trippe and B. Li, *Biochemistry*, 2022, **61**, 2159–2164.
32 C. T. Walsh, R. V. O'Brien and C. Khosla, *Angew. Chem., Int. Ed.*, 2013, **52**, 7098–7124.
33 C. Makris, J. R. Carmichael, H. Zhou and A. Butler, *ACS Chem. Biol.*, 2022, **17**, 3140–3147.
34 C. Makris, J. K. Leckrone and A. Butler, *J. Nat. Prod.*, 2023, **86**, 1770–1778.
35 Y. Sung, B. W. Miller and E. W. Schmidt, *Org. Lett.*, 2025, **27**, 1774–1778.
36 S. W. Fuchs, A. Proschak, T. W. Jaskolla, M. Karas and H. B. Bode, *Org. Biomol. Chem.*, 2011, **9**, 3130.
37 H. B. Bode, D. Reimer, S. W. Fuchs, F. Kirchner, C. Dauth, C. Kegler, W. Lorenzen, A. O. Brachmann and P. Grün, *Chem. Eur. J.*, 2012, **18**, 2342–2348.

38 Q. Zhou, A. Dowling, H. Heide, J. Wöhnert, U. Brandt, J. Baum, R. ffrench-Constant and H. B. Bode, *J. Nat. Prod.*, 2012, **75**, 1717–1722.
39 S. W. Fuchs, C. C. Sachs, C. Kegler, F. I. Nollmann, M. Karas and H. B. Bode, *Anal. Chem.*, 2012, **84**, 6948–6955.
40 D. Reimer, K. N. Cowles, A. Proschak, F. I. Nollmann, A. J. Dowling, M. Kaiser, R. ffrench-Constant, H. Goodrich-Blair and H. B. Bode, *ChemBioChem*, 2013, **14**, 1991–1997.
41 S. W. Fuchs, F. Grundmann, M. Kurz, M. Kaiser and H. B. Bode, *ChemBioChem*, 2014, **15**, 512–516.
42 Y.-M. Shi, M. Hirschmann, Y.-N. Shi, S. Ahmed, D. Abebew, N. J. Tobias, P. Grün, J. J. Crames, L. Pöschel, W. Kuttenlochner, C. Richter, J. Herrmann, R. Müller, A. Thanwisai, S. J. Pidot, T. P. Stinear, M. Groll, Y. Kim and H. B. Bode, *Nat. Chem.*, 2022, **14**, 701–712.
43 O. Schimming, F. Fleischhacker, F. I. Nollmann and H. B. Bode, *ChemBioChem*, 2014, **15**, 1290–1294.
44 X. Bian, A. Plaza, F. Yan, Y. Zhang and R. Müller, *Biotechnol. Bioeng.*, 2015, **112**, 1343–1353.
45 G. Wang, Z. Zhao, J. Ke, Y. Engel, Y.-M. Shi, D. Robinson, K. Bingol, Z. Zhang, B. Bowen, K. Louie, B. Wang, R. Evans, Y. Miyamoto, K. Cheng, S. Kosina, M. De Raad, L. Silva, A. Luhrs, A. Lubbe, D. W. Hoyt, C. Francavilla, H. Otani, S. Deutsch, N. M. Washton, E. M. Rubin, N. J. Mouncey, A. Visel, T. Northen, J.-F. Cheng, H. B. Bode and Y. Yoshikuni, *Nat. Microbiol.*, 2019, **4**, 2498–2510.
46 A. Tietze, Y. Shi, M. Kronenwerth and H. B. Bode, *ChemBioChem*, 2020, **21**, 2750–2754.
47 A. Proschak, P. Lubuta, P. Grün, F. Löhr, G. Wilharm, V. De Berardinis and H. B. Bode, *ChemBioChem*, 2013, **14**, 633–638.
48 Q. Zhou, F. Grundmann, M. Kaiser, M. Schiell, S. Gaudriault, A. Batzer, M. Kurz and H. B. Bode, *Chem. Eur. J.*, 2013, **19**, 16772–16779.
49 L. Zhao, R. M. Awori, M. Kaiser, J. Groß, T. Opatz and H. B. Bode, *J. Nat. Prod.*, 2019, **82**, 3499–3503.
50 M. Kronenwerth, K. A. J. Bozhüyük, A. S. Kahnt, D. Steinhilber, S. Gaudriault, M. Kaiser and H. B. Bode, *Chem.–Eur. J.*, 2014, **20**, 17478–17487.
51 S. A. Sieber and M. A. Marahiel, *Chem. Rev.*, 2005, **105**, 715–738.
52 C. Kegler, F. I. Nollmann, T. Ahrendt, F. Fleischhacker, E. Bode and H. B. Bode, *ChemBioChem*, 2014, **15**, 826–828.
53 M. F. Freeman, C. Gurgui, M. J. Helf, B. I. Morinaka, A. R. Uria, N. J. Oldham, H.-G. Sahl, S. Matsunaga and J. Piel, *Science*, 2012, **338**, 387–390.
54 B. I. Morinaka, A. L. Vagstad, M. J. Helf, M. Gugger, C. Kegler, M. F. Freeman, H. B. Bode and J. Piel, *Angew. Chem., Int. Ed.*, 2014, **53**, 8503–8507.
55 B. I. Morinaka, M. Verest, M. F. Freeman, M. Gugger and J. Piel, *Angew. Chem., Int. Ed.*, 2017, **56**, 762–766.
56 B. I. Morinaka, A. L. Vagstad and J. Piel, in *Methods in Enzymology*, ed. B. S. Moore, Academic Press, 2018, vol. 604, pp. 237–257.
57 F. Li, Z. Lin, P. J. Krug, J. L. Catrow, J. E. Cox and E. W. Schmidt, *Proc. Natl. Acad. Sci. U. S. A*, 2023, **120**, e2305575120.
58 H. Gross, V. O. Stockwell, M. D. Henkels, B. Nowak-Thompson, J. E. Loper and W. H. Gerwick, *Chem. Biol.*, 2007, **14**, 53–63.
59 D. S. May, C. M. Crnkovic, A. Krunic, T. A. Wilson, J. R. Fuchs and J. E. Orjala, *ACS Chem. Biol.*, 2020, **15**, 758–765.
60 I. M. Chauvin, L. J. Davis, A. Krunic and J. Orjala, *J. Nat. Prod.*, 2026, **89**, 573–583.
61 S. A. C. Figueiredo, M. Preto, G. Moreira, T. P. Martins, K. Abt, A. Melo, V. M. Vasconcelos and P. N. Leão, *Angew. Chem., Int. Ed.*, 2021, **60**, 10064–10072.
62 C. S. McCaughey, J. A. van Santen, J. J. J. van der Hooft, M. H. Medema and R. G. Linington, *Nat. Chem. Biol.*, 2022, **18**, 295–304.
63 L. Zaroubi, B. S. Paulo, E. Fung, H. Cavanagh, R. Britton, A. S. Eustaquio and R. G. Linington, *ACS Chem. Biol.*, 2025, **20**, 2393–2403.
64 C. H. Fergusson, J. Saulog, B. S. Paulo, D. M. Wilson, D. Y. Liu, N. J. Morehouse, S. Waterworth, J. Barkei, C. A. Gray, J. C. Kwan, A. S. Eustaquio and R. G. Linington, *Chem. Sci.*, 2024, **15**, 8089–8096.
65 T. C. E. Liebergesell and A. W. Puri, *Methods Enzymol.*, 2024, **702**, 215–227.
66 W.-L. Ng and B. L. Bassler, *Annu. Rev. Genet.*, 2009, **43**, 197–222.
67 M. Whiteley, S. P. Diggle and E. P. Greenberg, *Nature*, 2017, **551**, 313–320.
68 D. A. Jr. Cummings, A. I. Snelling and A. W. Puri, *ACS Chem. Biol.*, 2021, **16**, 1332–1338.
69 M. Wallace, D. A. Cummings Jr., A. G. Roberts and A. W. Puri, *mBio*, 2024, **15**, e01999–23.
70 I. J. Schalk, *Nat. Rev. Microbiol.*, 2025, **23**, 24–40.
71 Z. L. Reitz, M. Sandy and A. Butler, *Metallomics*, 2017, **9**, 824–839.
72 J. M. D. Robes, T. C. E. Liebergesell, D. G. Beals, X. Yu, W. J. Brazelton and A. W. Puri, *Proc. Natl. Acad. Sci. U. S. A*, 2025, **122**, e2507323122.
73 J. M. D. Robes, T. C. E. Liebergesell, V. P. Medvedeva and A. W. Puri, *mBio*, 2026, e03391.
74 L.-F. Nothias, D. Petras, R. Schmid, K. Dührkop, J. Rainer, A. Sarvepalli, I. Protsyuk, M. Ernst, H. Tsugawa, M. Fleischauer, F. Aicheler, A. A. Aksenov, O. Alka, P.-M. Allard, A. Barsch, X. Cachet, A. M. Caraballo-Rodriguez, R. R. Da Silva, T. Dang, N. Garg, J. M. Gauglitz, A. Gurevich, G. Isaac, A. K. Jarmusch, Z. Kameník, K. B. Kang, N. Kessler, I. Koester, A. Korf, A. Le Gouellec, M. Ludwig, C. M. H, L.-I. McCall, J. McSayles, S. W. Meyer, H. Mohimani, M. Morsy, O. Moyne, S. Neumann, H. Neuweger, N. H. Nguyen, M. Nothias-Esposito, J. Paolini, V. V. Phelan, T. Pluskal, R. A. Quinn, S. Rogers, B. Shrestha, A. Tripathi, J. J. J. van der Hooft, F. Vargas, K. C. Weldon, M. Witting, H. Yang, Z. Zhang, F. Zubeil, O. Kohlbacher, S. Böcker, T. Alexandrov, N. Bandeira, M. Wang and P. C. Dorrestein, *Nat. Methods*, 2020, **17**, 905–908.
75 M. A. Tammam, F. Pereira, E. Skellam, S. Bidula, A. Ganesan and A. El-Demerdash, *Nat. Prod. Rep.*, 2025, **42**, 788–841.
76 A. Cutignano, G. Cimino, G. Villani and A. Fontana, *ChemBioChem*, 2009, **10**, 315–322.

